

Panchromatic Fourier Transform Spectrometer (PanFTS) for Geostationary Measurements of Atmospheric Composition

S. Sander, D. Bekker, J.-F. Blavier, M. Heverly, R. Key, K. Manatt, D. Rider, A. Wu, Y-H Wu and F. Zhong

Jet Propulsion Laboratory, California Institute of Technology.
4800 Oak Grove Drive
Pasadena, CA 91109 USA

Abstract: The Panchromatic Fourier Transform Spectrometer (PanFTS) instrument is being developed, to meet the science demands of measuring a wide range of trace gases with unprecedented vertical resolution, by sensing the UV, visible, and IR in one instrument. In the development and demonstration of the PanFTS breadboard instrument, significant progress has been made in the areas of optical design for wideband spectral grasp, focal planes and readouts with in-pixel and on-chip readouts, and a long-life, cryogenic optical path difference mechanism for the interferometer.

I. THE NASA GEO-CAPE MISSION

Geostationary Coastal and Air Pollution Events (GEO-CAPE) is a space mission recommended by the U.S. National Research Council as part of the Earth Science Decadal Survey [1]. GEO-CAPE and GACM (Global Atmospheric Composition Mission) are the two missions recommended by the NRC for comprehensive atmospheric trace gas measurements from geostationary and low-earth orbits, respectively. From its unique geostationary perspective near 100° W. longitude, GEO-CAPE will offer unprecedented measurements of the spatial and temporal variabilities of trace gases and aerosols that influence air quality and climate change over North America from 10° N. to 60° N. latitude. In combination with chemistry-transport models, GEO-CAPE measurements will enable the determination of natural and anthropogenic emissions of pollutants and trace gases that result in the formation of tropospheric ozone and aerosols. These data products will be extremely valuable to the research community and to operational agencies such as NOAA and USEPA which are responsible for developing effective air pollution mitigation strategies.

The Science Working Group for the GEO-CAPE mission is in the process of refining a Science Traceability Matrix (STM) which defines the flow-down of requirements from the top-level scientific questions to measurements. For the atmospheric component of the mission, the mission-critical trace gas measurements include ozone (O₃), carbon monoxide

(CO), aerosols, nitrogen dioxide (NO₂) and sulfur dioxide (SO₂). For O₃ and CO, the measurement requirements call for the ability to retrieve vertical mixing ratio profiles with two independent pieces of information in the troposphere, including sensitivity to the planetary boundary layer. This profile information is required to diagnose human and ecosystem exposure to elevated pollutant concentrations near the surface, to trace the long-range transport of pollutants on continental scales, and to properly assess the radiative forcing of ozone in the middle troposphere. Highly desirable measurements include formaldehyde (HCHO), methane (CH₄), ammonia (NH₃), glyoxal (CHOCHO), and other aerosol properties. The required spatial footprint dimension is 4x4 km and the temporal repeat cycle is 1-2 hours.

II. PANCHROMATIC FOURIER TRANSFORM SPECTROMETER (PANFTS) FOR GEO-CAPE

The Panchromatic Fourier Transform Spectrometer is a NASA Earth Science Technology Program-funded development to demonstrate an instrument capable of meeting or exceeding GEO-CAPE atmospheric science requirements. The PanFTS flight instrument design combines measurement capabilities for the 0.26-15 μm spectral range in a single package. The wide spectral coverage is important for retrieving the entire suite of GEO-CAPE target molecules, including several in widely different wavebands. Measurement of the same species in different spectral regions significantly enhances the information content of the vertical profile retrievals [2].

The PanFTS design combines a conventional Michelson interferometer with several unique features. The PanFTS instrument is a hybrid based on spectrometers like TES (Tropospheric Emission Spectrometer) that measures thermal emission, and those like OCO (Orbiting Carbon Observatory) and OMI (Ozone Monitoring Instrument) that measure scattered solar radiation. As such the PanFTS design has two parallel optical trains, one for infrared wavelengths and one for UV-Vis. The beam aperture of 5 cm is driven by the Rayleigh criterion to resolve the ground pixels. The

instrument temperature is 180 K to make the instrument self emission negligible compared to the Earth's emission.

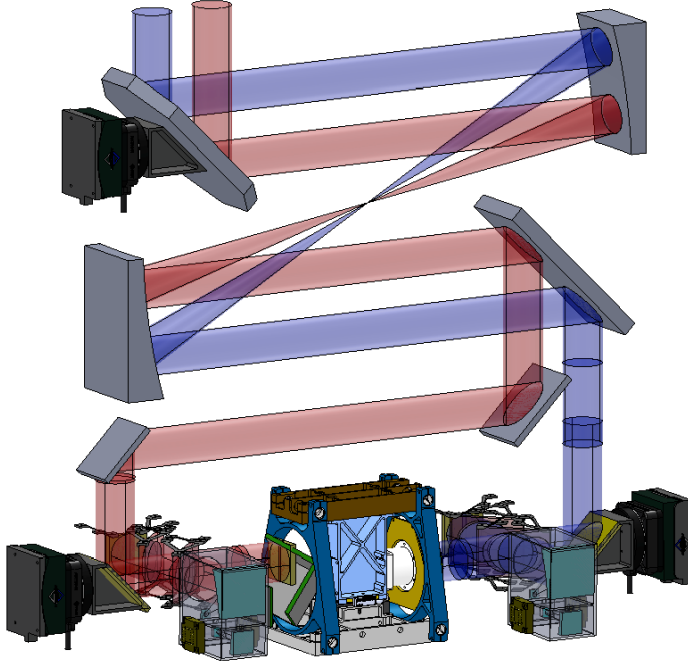


Fig 1. The PanFTS flight instrument optical design

Simultaneous measurements over the broad spectral range are accomplished by a two sided interferometer with separate optics and FPAs for the UV-visible and IR spectral domains. This allows the instrument design to be independently optimized for both spectral domains. The overall design is compact because the two sides share a common set of fore optics, and a single common interferometer optical path difference mechanism (OPDM) and metrology laser as well as a number of other instrument systems including the line-of-sight pointing mirror, the data management system, thermal control system, electrical system, and the mechanical structure. The PanFTS breadboard instrument being tested in the laboratory is demonstrating basic functionality for simultaneous measurements in the visible and IR.

A. Optical Design

The PanFTS optical design for a notional flight instrument is shown in Fig. 1. Radiation enters the instrument at the top via a two axis gimbaled line-of-sight pointing system like the one used on TES. It directs two parallel 5 cm optical beams that share unity magnification foreoptics. The IR and UV-Vis beams never overlap in the foreoptics so each mirror has a separate IR zone coated with gold and a UV-Vis zone coated with UV enhanced aluminum. The fore optics, which includes a field stop to eliminate off-axis radiation, terminates with fold mirrors which send the long and short-wavelength beams into their respective side of the interferometer that is optimized for each spectral domain. The UV-visible side of the interferometer is in the bottom right of Fig. 1. The design is the same as the Fourier Transform Ultraviolet Spectrometer (FTUVS) at JPL's Table Mountain

Facility [3] and uses ordinary flat mirrors to achieve the required throughput and wavefront quality ($\lambda/25 @ 0.633 \mu\text{m}$). The IR side of the interferometer is in the bottom left of Fig. 1. Its design uses double pass cube corner optics as in JPL's Mark IV balloon interferometer [4]. Both sides share the common OPDM in the bottom middle of Fig. 1 which enables simultaneous co-located IR and UV-Vis measurements of a scene. Each optical train has a 5 cm beam diameter at the beamsplitter, yielding an etendue of $7.8 \times 10^{-11} \text{ meter}^2 \text{ steradian}$ for each detector pixel. Because the IR and UV-Vis optical paths are separate in the interferometer conventional materials and coatings are used. The IR path uses a ZnSe beamsplitter and compensator, and gold for the optics coating like TES. The UV/Vis path uses a CaF_2 beamsplitter and compensator, and UV-enhanced aluminum for mirror coating like OMI.

In the UV-Vis side of the interferometer, the zero path difference position is in the middle of the range of travel which increases the UV-Vis SNR because the equivalent of two spectral scans are recorded, while the IR side of the interferometer is recording just one. The IR side uses cube corners which are insensitive to tip/tilt errors so a dynamic alignment system isn't needed for the IR side. To prevent shear errors caused by cross-axis motion of the moving mirror, the IR beam is double-passed as in the MkIV interferometer. This enables the optical beam to traverse a distance four times the mechanical motion of the OPDM. The required mechanical travel and velocity of the OPDM are halved. The 10 cm optical path difference is achieved with just $\pm 1.25 \text{ cm}$ of mechanical motion (half the breadboard instrument mechanical motion).

The key concepts of the PanFTS design have been tested in a breadboard implementation in which the optical elements are mounted on a standard optical table. The stability of the OPDM servo can be probed with the fringes of the He:Ne metrology laser and the velocity was measured as constant to 1% RMS.

B. Optical Path Difference Mechanism (OPDM)

The PanFTS interferometer OPDM is shown in Fig. 2 (without the IR cube corner attached). The OPDM simultaneously controls the optical path difference for the visible and IR sides of the interferometer. The four bar linkage mechanical design uses rotational spring flex pivots at each link and is driven by a non-contacting linear voice coil actuator with of a magnet fixed to the base and a coil that move the upper part of the mechanism. The flex pivots are rated for infinite life because the flexing angles are so small. The design has no moving contact surfaces so there are no lubricant or mechanical wear out risks. An optical encoder with 5 nm resolution provides accurate and repeatable position data. Autocollimator based tests to make fringe contrast measurements with the OPDM installed in the breadboard interferometer show that the mechanism exceeds the tip/tilt specification by a large margin with a very low maximum tip/tilt error of less than $50 \mu\text{rad}$. On the visible side of the interferometer this tip/tilt error is corrected by a piezo actuated tip/tilt stage using a fiber fed metrology laser to measure

tip/tilt via the phase of three small sections of the laser beam as an error signal to remove this residual error. The metrology laser is also digitized simultaneously with the FPA outputs to provide precise mirror translation information.

The OPDM system is being tested under simulated space conditions in order to demonstrate the stability and reliability of the design. One of the OPDM mechanisms is currently cycling full travel (0 mm - 50 mm), under -100°C simulated mission conditions. We intend to continue this test for 2.5 million cycles to assess OPDM durability. The test system allows control of the piezo mechanism throughout its full range. Data from the piezo tests as well as stage precision and smoothness are collected by an optical quadcell system. A 632 nm helium-neon reference laser is targeted onto the OPDM plane mirror which is articulated by a piezo-actuated tip/tilt stage. The return beam is split off from the initial path and aligned onto the quad cell. This allows fine measurement of the tip / tilt of the OPDM optical system. As this system is mounted outside of our LN2 cooled thermal chamber, adjustments were made for alignment as the chamber system was cooled. The thermal system is monitored and under control of a Labview-based system. Temperature, pressure and electronic parameters are monitored and recorded. The OPDM structure is monitored by several type-T thermocouples. Email alarms are generated for out of range values. The system is automatically shut down safely should there be a power failure or unexpected temperature excursion. This safing is accomplished by secondary control systems. The collected data archive will be analyzed to assess the effects of the space thermal and vacuum environment on the OPDM system.

C. Focal Plane Arrays

The PanFTS breadboard instrument has two focal plane arrays located in separate opto-mechanical assemblies that receive collimated, interferometrically-modulated radiation from each side of the interferometer. An advantage of an imaging FTS is that a very high throughput is possible because the detectors are not required to lie within the central fringe of the "bull's-eye" interference pattern. Additional fringes can be used, until they become narrower than the detector pixels (or until off-axis aberrations exceed the pixel size). Using four FPAs to cover the spectral range allows the individual beam trains to be optimized for maximum performance in each spectral domain. The interferometer outputs on both sides are individually imaged onto two FPAs by conventional focusing optics.

The visible spectral region employs a custom 4 x 4 pixel focal plane assembly with an on-chip two stage sigma-delta analog-to-digital converter for each pixel (Fig. 3). The converters share a common clock so that all pixels are digitized simultaneously. The detector readout integrated circuit (ROIC) is fabricated in CMOS and is hybridized to a silicon PIN diode array fabricated by Teledyne Imaging Systems. The PIN diode array is hybridized to the ROIC using indium bump bonds. The pixels are $60\ \mu\text{m} \times 60\ \mu\text{m}$. The sigma-delta outputs are read by an FPGA where the sigma-

delta ADC outputs are filtered and decimated to the desired frame rate, bandwidth and precision. The array easily achieves the required 16 kHz frame rate (8 kHz bandwidth) with 16 bits of precision.



Fig. 2. The PanFTS Instrument Optical Path Difference Mechanism

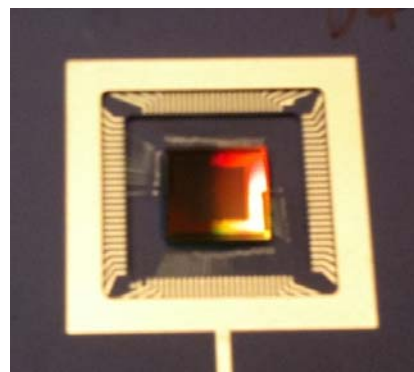


Fig. 3. PanFTS 4x4 pixel silicon FPA with on-chip sigma-delta ADCs.

The IR FPA is a commercially available InSb CMOS array with 256 x 256 pixels from Raytheon Vision Systems. It is capable of the required frame rate at a lower spatial coverage (windowed mode) and of the required spatial coverage at a lower frame rate. It is an InSb device that needs cooling with LN2 down to 77 K.

D. FPA Control and Data Handling

The FPA clocking and control are handled by a Xilinx ML507 development board. This board is a very convenient FPGA prototyping platform as it provides readily accessible user I/O as well as various on-board peripherals (memory, UART, Ethernet, and others). The digitization of the FPA output is done by a pair of Analog Devices AD9446 ADCs on separate development boards. These 16-bit ADCs are capable of running at up to 100 MHz, which is more than a sufficient sampling rate to handle FPA output. User commands to the system are handled over an RS232 serial link.

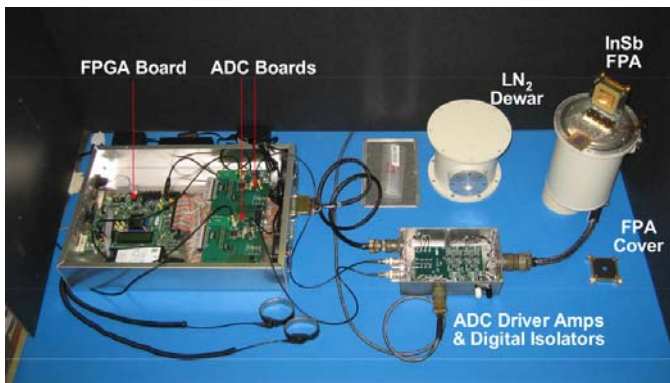


Fig. 4. Photo showing FPGA, ADCs, interface board and the IR FPA.

The IR FPA operates with voltages that do not conform to any interface standard. A custom built interface board sits in between the FPA and FPGA/ADC development boards and performs the necessary level translation and amplification. Isolators are used to suppress the noise induced by the digital lines from the FPGA on the analog outputs of the FPA [5].

With its on-chip sigma-delta ADCs, the visible FPA provides an all-digital interface to the FPGA acquisition system. A Sinc-cubed filter followed by a differentiator / decimator are implemented on the FPGA and applied to the output of the UV-Vis FPA. The filter output is a 16-bit-per-pixel data stream. This data stream is combined with pixel data produced by the IR FPA, sent over Ethernet to a host computer, and displayed in real-time using Matlab.

Both the IR and UV-Vis focal plane arrays are sampled at constant frame rate. The metrology laser fringes are detected and digitized separately in the IR and visible interferometers, using the same time base as the imaging arrays so that we can convert the time-domain interferograms to optical path difference [6].

ACKNOWLEDGMENTS

Support from the NASA Instrument Incubator Program is gratefully acknowledged. The research described in this publication was carried out at the Jet Propulsion Laboratory, California Institute of Technology under a contract with the National Aeronautics and Space Administration. Copyright 2011, California Institute of Technology. Government sponsorship acknowledged.

REFERENCES

- [1] National Research Council, *Earth Science and Applications from Space: National Imperatives for the Next Decade and Beyond*, National Academies Press, Washington, D.C., 2007.
- [2] A. Eldering et al., *PanFTS: Panchromatic measurements for unprecedented vertical sensitivity and temporal resolution of trace gases*, Hyperspectral Imaging and Sounding of the Environment (HISE) Topical Meeting, Optical Society of America, Toronto, July, 2011
- [3] Cageao, R. P.;Blavier, J.-F.;McGuire, J. P.;Jiang, Y.;Nemtchinov, V.;Mills, F. P.; Sander, S. P. High-Resolution Fourier-Transform Ultraviolet-Visible Spectrometer for the Measurement of Atmospheric Trace Species: Application to OH, *Appl. Opt.*, vol. 40, p. 2024, 2001.

- [4] Toon, G. C. The JPL Mark IV Interferometer, *Optics and Photonics News*, vol. 2, p. 19, 1991.
- [5] Bekker, D., Blavier, J.-F., Key, R., Rider, D., and Sander, S., "An FPGA-based Focal Plane Array Interface for the Panchromatic Fourier Transform Spectrometer," in *Aerospace Conference*, 2011 IEEE, March 2011, pp. 1-10.
- [6] Campbell, J., "Synthetic quadrature phase detector/demodulator for fourier transform spectrometers," *Appl. Opt.*, vol. 47, pp. 6889-6894, 2008.